Check for updates

Evaluation of pretreatment and membrane configuration for pressure-retarded osmosis application to produced water from the petroleum industry

Dareen Dardor [a], Mashael Al Maas [a], Joel Minier-Matar [a], Arnold Janson [a], Ahmed Abdel-Wahab [b], Ho Kyong Shon [c], Samer Adham [a,d,*]

[a] *ConocoPhillips Global Water Sustainability Center, Qatar Science & Technology Park, Doha, Qatar*
[b] *Chemical Engineering Program, Texas A&M University at Qatar, Doha, Qatar*
[c] *Center for Technology in Water and Wastewater, University of Technology Sydney, Ultimo, New South Wales, Australia*
[d] *Center for Advanced Materials, Qatar University, Doha, Qatar*

HIGHLIGHTS

- PRO evaluation on hypersaline produced water (PW) from the petroleum industry
- Real PW from different oil production sites was used for testing.
- Several levels of pretreatment including physical and physicochemical processes
- PW can be treated to suitable levels for PRO application to avoid membrane fouling.
- Novel hollow-fibers are less prone to fouling compared to flatsheet membranes.

GRAPHICAL ABSTRACT
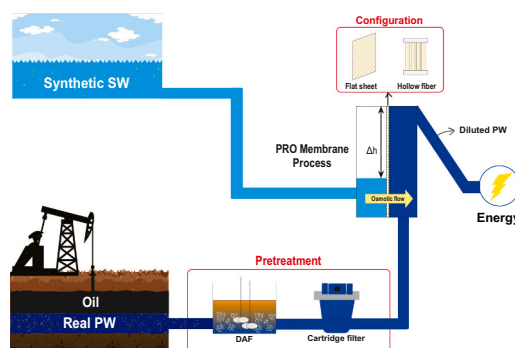
ARTICLE INFO

ABSTRACT

Pressure-retarded osmosis (PRO) is a promising membrane technology for harnessing the osmotic energy of saline solutions. PRO is typically considered with seawater/river water pairings however greater energy can be recovered from hypersaline solutions including produced water (PW) from the petroleum industry. One of the major challenges facing the utilization of hypersaline PW is its high fouling propensity on membranes. In this unique experimental evaluation, real PW from different sites was pretreated to varying degrees: i) minimal, ii) intermediate, and iii) extensive. The treated effluent was subsequently used for PRO testing and fouling rates were assessed for different membrane configurations over multiple cycles. Commercial grade flat sheet (FLS) coupons and novel hollow fiber (HF) modules were compared to validate the lower fouling propensity of HF membranes in PRO application. When minimally pretreated PW (10-micron cartridge filtration (CF)) was tested in FLS mode, severe membrane fouling occurred and the PRO flux decreased by 60%. In contrast, HF modules showed <1% flux decrease under both minimal and intermediate pretreatment schemes. Extensive pretreatment (1-micron CF, dissolved air flotation (DAF), powdered activated carbon, and microfiltration) reduced FLS PRO

---

* Corresponding author at: Center for Advanced Materials, Qatar University, Doha, Qatar.
  E-mail address: sadham@qu.edu.qa (S. Adham).

flux decline to <1%. These results confirm that PW can be treated to suitable levels for PRO application to avoid membrane fouling. Further validation of these pretreatment methods requires long term pilot testing and techno-economic assessment.

1. Introduction

1.1. Background

With increasing energy demand due to the rapid population growth, and higher risks of climate change, research efforts have focused on renewable energy and lower carbon footprint technologies [1,2]. One abundant source of energy is the osmotic energy available when solutions of different salinities are separated by a membrane [3,4]. Several technologies are available for harnessing potential osmotic energy and converting salinity gradients into useful work including; pressure-retarded osmosis (PRO) [5–7], reverse electrodialysis [8,9], and capacitive mixing [10,11]. Among these technologies, PRO has been the most widely investigated. In PRO, a low salinity feed solution (FS) is separated from a higher salinity draw solution (DS) by a semi-permeable membrane which allows only solvent molecules to pass through [12]. By natural osmosis, water molecules from the low salinity feed are drawn through the membrane to the higher salinity side until chemical equilibrium is reached. If the DS side is under restricted volume conditions, this flow of water causes an increase in the hydraulic pressure on the draw side. The resulting pressurized flow of diluted DS can then be used to generate power via hydroturbines in a way similar to conventional hydro-power plants or converted directly into mechanical work by pressure exchangers [13,14].

Thus far, PRO research has focused on membrane development and mass transfer modeling [15–20]. There have also been several pilot scale studies conducted including those by the Norwegian company Statkraft, the Mega-ton project in Japan, and the GMVP project in Korea (here, G is for global, M is for membrane distillation, V is for valuable resource recovery, and P is for PRO) [21–25]. In a more recent study, Binger et al. performed experimental evaluations of a pilot scale seawater reverse osmosis (SWRO) system integrated with PRO to reduce overall energy requirements of SW desalination. The DS used was RO concentrate and FS was municipal tap water. Specific energy requirements for the overall process were found to be greater than that recovered by PRO [26]. All these studies focused on SW/freshwater pairings have proven to be to be not economically viable for various applications due to an insufficient salinity gradient [27,28]. This is because the specific energy recoverable from this pairing is generally less than the energy inputs needed after considering process inefficiencies. An alternative salinity gradient with much higher osmotic energy is the hypersaline produced water (PW)/ SW pairing. PW is the water extracted with hydrocarbons from oil and gas (O&G) reservoirs and represents the largest volume waste stream in O&G operations [29]. PW from oilfield operations can have salinities as high as 300 g/L [30–32]. Although this hypersalinity hinders the availability of PW for reuse, it represents a huge amount of stored potential energy that could be harnessed through PRO.

This PW/SW pairing can be used to either recover energy or to produce water for use in secondary oil recovery operations. In the latter case, the water drawn through the PRO membrane adds to the volume of water injected into the geological formation resulting in higher oil flow at the producing well. When PRO is used for waterflooding operations, the product is not energy but oil, a more valuable commodity; a net economic benefit of over $70,000/yr per 8″Ø × 40″ PRO membrane has been projected [33]. Another example of a high salinity gradient application is salt mining and the work undertaken by SaltPower in Denmark. In this application, high salinity groundwater serves as the DS to produce electricity; the FS can be either low salinity surface water or another process stream from salt mining operations [34].

Several challenges face hypersaline PRO applications including the development of mechanically strong membranes that are not susceptible to concentration polarization effects and the implementation of effective pretreatment technologies that can minimize membrane fouling. When using PW, suitable pretreatment is essential to enable stable operation in any membrane application. Although there are many publications evaluating the fouling of PRO membranes and pretreatment methods, these studies focused on SW, river water, and/or treated sewage effluent streams with limited work on PW from the petroleum industry [35–41]. J. Ju et al. evaluated the effect of feed water quality and pretreatment strategies on PRO flux and power density. They tested the efficiency of a wide range of filtration technologies for treating effluent from a real wastewater treatment plant as a potential PRO FS. Their results confirm that organic matter present in the water greatly affects PRO fouling [42]. Yip and Elimelech also presented a study focused on the effect of organic fouling on PRO performance using model river water containing natural organic matter as the FS. Severe membrane fouling and water flux decline were observed, confirming the huge impact that fouling has on the energy potential of PRO systems [43]. Thus, an evaluation of the pretreatment requirements and fouling mitigation strategies for PW use in PRO application is essential to enable unlocking the high salinity of these wastewater streams.

Both flat sheet (FLS) and hollow fiber (HF) membranes have been developed and used for PRO testing in various applications with each configuration having their own benefits and drawbacks [44–47]. While published experimental data has generally reported higher applied hydraulic pressure for FLS compared to HF membranes, there are several practical advantages to the use of HF modules for PRO, including:

- Higher packing density resulting in higher productivity per unit volume [48,49].
- No need for spacers as they are self-supported membranes [50,51].
- Reduced fouling propensity.

Although the first two advantages are practical considerations, the impact of configuration on membrane fouling in PRO application is not reported in literature. Other references have reported comparisons between FLS and HF fouling rates in different applications. For example, in a paper published by Howe et al. the team conducted side-by-side microfiltration and ultrafiltration experiments which proved that FLS membranes typically foul more rapidly than HF membranes under similar conditions [52]. In another evaluation, Minier-Matar et al. compared the fouling potential of FLS and HF membranes in forward osmosis application. In this evaluation, the results again showed that HF membranes had better flux and higher rejection compared to FLS membranes [53]. These studies indicate that HF membranes could also be less prone to fouling in PRO application; however experimental evaluations remain necessary to validate this claim.

1.2. Objectives

Based on the above, this study focused on comparing various levels of PW pretreatment for PRO application using different membrane configurations. Actual hypersaline PW from oil production operations was pretreated to varying degrees (minimal, intermediate, and extensive) by a combination of physical and/or physicochemical processes. The efficiency of these pretreatment technologies was then evaluated in PRO mode for both commercial grade FLS membranes and novel HF modules fabricated by the project team. To the authors' knowledge, this is the first evaluation of actual hypersaline PW pretreatment requirements for FLS and HF PRO membranes.

2. Materials & methods

2.1. Actual produced water samples

Hypersaline PW samples were obtained from different O&G operations in the United States. The samples were characterized upon receipt and stored at 4 °C to avoid changes in chemical composition. Water quality analyses were also conducted before and after each experiment for quality assurance purposes.

2.2. Synthetic seawater samples

Synthetic SW at 35 g/L salinity prepared from deionized water and sodium chloride was used for this evaluation. This decision was made to eliminate the interferences of organics present in actual SW that would result in fouling both sides of the PRO membrane. Extensive studies in literature already report SW testing and evaluations, including detailed pretreatment [54–57].

2.3. Chemicals

The following chemicals were used in this evaluation:

- Deionized (DI) water supplied by Milli-Q ultrapure water system (Integral 10, Millipore) at a resistivity of ≈18 MΩ-cm
- Sodium chloride (NaCl) at 99% purity, iron (III) chloride ($FeCl_3$) >97% purity, and steam activated charcoal (Norit), from Sigma-Aldrich
- Sodium hydroxide pellets (NaOH) from Thermo Fisher Scientific
- Biocide M-43 from Metito.

All chemicals were used as received without any modifications or treatment except for the powder activated charcoal (PAC) which was prepared according to the following procedure:

- Soaked in DI water for 1 h.
- Filtered through a 0.45 μm MF membrane (Sterlitech, USA) using vacuum filtration.
- Dried in the oven at 105 °C for 2 h before testing.

2.4. Laboratory analyses

Table 1 summarizes the analytical measurements and laboratory equipment used during this investigation.

2.5. Pretreatment technologies testing protocol

Different pretreatment technologies, selected based on team experience in PW treatment, were evaluated for the PRO DS (i.e. actual hypersaline oil-PW). The effectiveness of these technologies was measured through their ability to remove suspended solids and organics down to

Table 1
Analytical equipment.

Measurement	Instrument model
pH and conductivity	Orion 3-star meter, Thermo Scientific
Turbidity	Turbidimeter, Thermo Scientific
Total organic carbon (TOC), inorganic carbon (IC) and total nitrogen (TN)	TOC-V, Shimadzu
Total oil & grease (TOG)	Horiba OCMA-350 spectrophotometer
Dissolved ions	Ion chromatography, ICS 6000, Thermo Scientific
Total elements	Inductively coupled plasma (ICP), ICAP 6500, Thermo Scientific
Fourier-transform infrared (FTIR) spectroscopy	Nicolet 6700 FT-IR spectrometer
Surface appearance	Nikon camera D5300 24 MP

suitable levels that minimize PRO membrane fouling. The pretreatment technologies selected include:

- *Coagulation and dissolved air flotation (DAF):* the coagulation protocol was developed based on conditions reported in literature with $FeCl_3$ as the primary coagulant [58]. First, 120 mg/L of $FeCl_3$ was added to 1.5 L of PW in a 2 L jar tester and the pH adjusted to 8.5 using a 5 M NaOH solution. After stirring for 10 min, ≈500 mL of air-saturated DI water pressurized at 40 bar was introduced targeting a 25% dilution of the PW. The solution was left to separate for 15 min, and the pretreated PW sample was collected using the jar tester drainage valve. These basic DAF testing conditions were optimized in subsequent treatment evaluations for the specific water quality being tested. Platypus 4G Jar Tester was used for this evaluation with DAF test accessories No. 4GSAT and 4GCOPM (Australian Scientific Pty).
- *Cartridge filtration (CF):* following DAF treatment, CF was applied to improve the removal of suspended solids and organics. Two CF sizes, 1- and 10-μm, were evaluated (LP Grade 30 and 50 respectively, Parker). TOC analyses were conducted on filtered samples for performance comparison.
- *Powdered activated carbon (PAC) and microfiltration (MF):* adsorption using PAC followed by MF was applied as the final polishing step for the removal of dissolved organics. Different PAC dosages of 250, 500, and 750 mg/L were evaluated along with a control sample (i.e. PAC dosage of 0 mg/L). For the dosage optimization study, 100 mL PW after DAF and CF treatment was added to each 250 mL glass Erlenmeyer flask having the weighed amounts of PAC. The mixtures were then stirred for 1 h at 200 rpm using a VWR Scientific Advanced Orbital Shaker, Model 3500. The solutions were then left to settle for 30 min before applying MF vacuum filtration using a 0.45 μm membrane. TOC analysis was conducted on treated samples for performance tracking.

2.6. Pretreatment schemes

Three different PW pretreatment schemes of varying extents (minimal, intermediate, and extensive) were evaluated for the pretreatment of the PRO DS (Fig. 1).

2.7. Bench-scale PRO setup

The bench scale PRO system (Fig. 2) consists of two closed loops, one for the FS and the other for the DS. The feed loop, made of plastic (PFA tube, Swagelok, USA), consists of a variable speed pump (KNF, Switzerland) used to generate crossflow across the membrane cell (SEPA CF II, Sterlitech, USA) and is capable of operating up to 7 bar pressure. The DS loop consists of a high-pressure pump (Hydracell, USA) where the DS recirculates through the cell at pressures up to 70 bar. The flow rate in this loop is kept constant at different pressures using a PID controller embedded within the control system (cRIO-9039, NI, USA). Key process parameters, temperature, pressure, flowrates, conductivities (feed/draw) and water flux are monitored and recorded by the control system. The water flux is calculated based on the change of the feed tank weight, monitored through an analytical balance (Meter Toledo, Switzerland). Both loops are temperature controlled using two water baths (Julabo, Germany). To avoid excessive dilution of the DS during the test, concentrated NaCl solution (3–5 M) is added via a dosing pump (KNF, Switzerland) until the conductivity reading reaches the target value. The unit is also flexible in operating under both FLS and HF modes.

2.8. PRO membranes and spacers

Both FLS and HF membranes were used for this evaluation. For the FLS mode, commercial thin film composite (TFC) PRO membranes were obtained from Toray industries Inc. (Japan). The membrane coupons
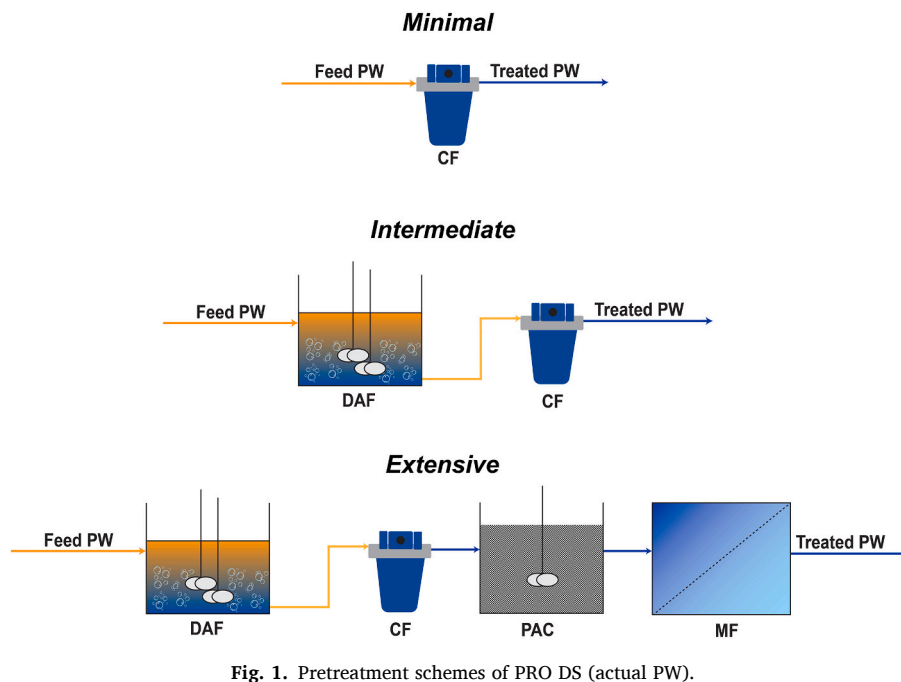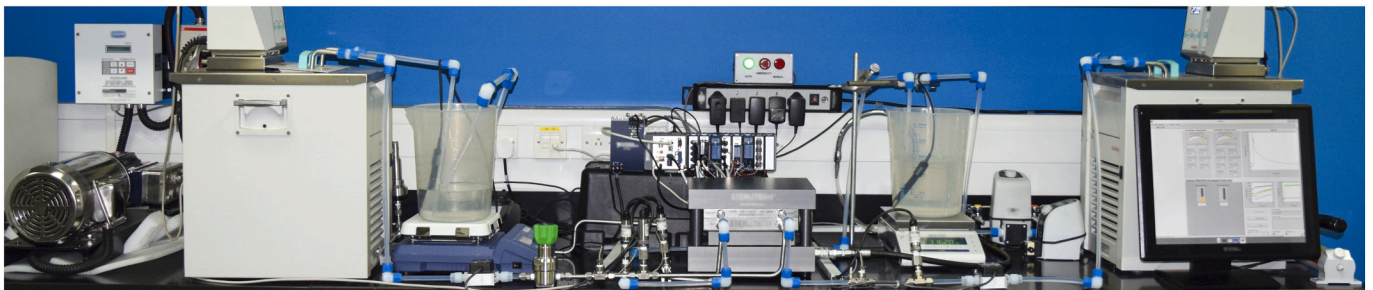
Minimal

Intermediate

Extensive

Fig. 1. Pretreatment schemes of PRO DS (actual PW).
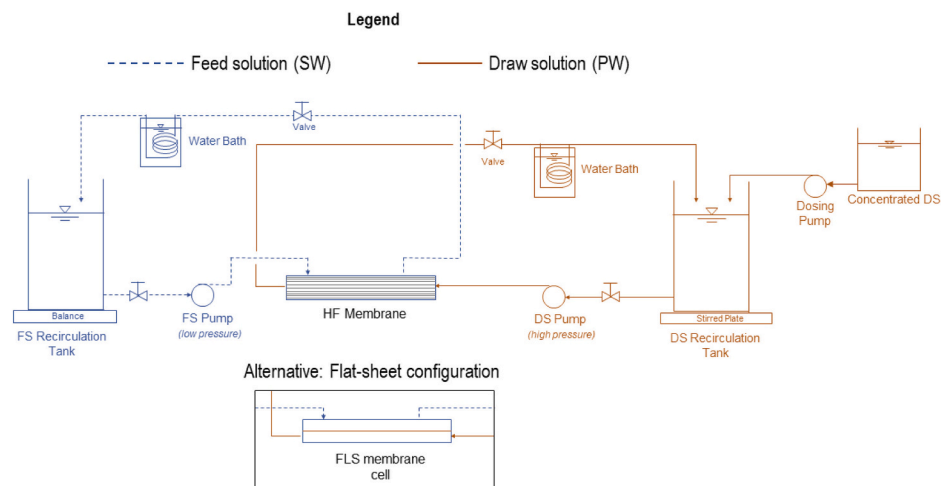
A)

B)

Fig. 2. PRO bench scale unit.
A) Photo. B) Schematic.

were loaded to the unit with the active layer facing the high-pressure DS side and the support layer facing the low-pressure FS side. In the feed channel, a standard Sterlitech skim plate and two SEPA CF permeate carriers were used while the draw side had a SEPA CF medium foulant spacer (47 mil). The edges of each membrane were covered with water-resistant tape on the active layer side to prevent membrane damage around the O-ring facing the high-pressure DS [59]. The average effective membrane area of the tested coupons was around 120 cm^2.

Novel PRO HF TFC membranes with a polyethersulfone (PES) support layer and a polyamide (PA) active layer were prepared by the project team and used in this comparative pretreatment evaluation. The PA active layer was formed by interfacial polymerization (IP) method.

Outer surface of the membranes (PES support layer) was designed to be highly porous with an open pore structure to reduce internal concentration polarization effects through faster solvent transport. The hollow fibers were modulated for use in bench scale evaluations by assembling 5 fibers each [46]. During PRO testing, the high-pressure DS was facing the active layer (i.e., on the lumen side) and the low-pressure FS was facing the support layer (shell side). Table 2 summarizes the intrinsic properties of both FLS, and HF membranes used in this evaluation.

The water permeability (A) value of the FLS membrane was higher compared to the HF membrane, however its salt permeability (B) was also higher resulting in a higher B/A value. Other PRO membranes reported in literature have A values ranging between 0.5 and 3 LMH/bar, and B values between 0.2 and 0.6 LMH. The resulting B/A values are typically <1 and comparable to those reported in Table 2 for the membranes under evaluation [60–66]. The HF membrane tested is among the better performing range of membranes based on these B/A values, while the FLS membrane used had a relatively high B value which negatively affected its performance. Higher B/A values typically indicate that a membrane is more susceptible to internal concentration polarization effects as more salt passage and build-up takes place at the support layer. This phenomenon results in lower effective osmotic driving force and hence lower flux is expected for the FLS Toray membrane compared to the HF module being tested.

2.9. PRO performance evaluation

During all stages of the FLS evaluation, flowrates were kept constant at 600 mL/min on the DS side and 20 mL/min on the FS side. Prior to testing, the membranes were compacted by circulating DI water on both sides and gradually increasing the pressure on the DS side until the maximum intended pressure was reached. The unit was then left under pressure overnight for approximately 14 h and the stable DI water flux recorded. Under these conditions DI water permeates from the DS to the FS due to the applied hydraulic pressure (ΔP). Concentrated NaCl solution is then dosed to the DS until its salinity reaches the desired concentration (0.6 M, or 1 M NaCl). In this situation, $\Delta\pi$ becomes greater than ΔP and water permeates against the applied hydraulic pressure in PRO mode. The pressure is then decreased stepwise, and the average PRO water flux is recorded for 40 min intervals at each stage [59].

A similar procedure was followed for the HF membrane testing, except for 150 mL/min flowrates on both the FS and DS sides and membrane pre-stabilization for only 60 min instead of overnight compaction. These conditions are in agreement with previous evaluations conducted by the project team on novel HF membranes [46].

2.10. Power density calculation

Power density (PD) is a common performance metric for different PRO membranes and systems and is defined as the power produced per unit membrane area. PD can be determined experimentally as the product of the PRO water flux Jw and the applied hydraulic pressure (Eq. (1)).

$$PD = J_w \Delta P \tag{1}$$

Table 2
Intrinsic membrane properties.

Parameter	FLS Toray	Novel HF
Water permeability, A (LMH/bar)	2.33 ± 0.5	1.22 ± 0.12
Salt permeability, B (LMH)	1.77 ± 0.5	0.55 ± 0.05
B/A (bar)	0.76 ± 0.5	0.45 ± 0.05
Structural parameter, S (µm)	183 ± 40	770 ± 20
Area (cm²)	120	17.3
Material	TFC	TFC
Inner diameter/outer diameter (µm)	–	663/1050
Active layer	–	Lumen side

Experimental results of the PRO membrane performance were validated against predictions of published process models for FLS membranes [67,68]. For each test, the water and salt permeabilities were calculated and input in the model along with the operating conditions. Based on the outputs, the power density was calculated and compared to the experimental data.

2.11. PRO fouling test protocol

PRO fouling tests were conducted using both FLS and HF membranes. A new membrane was used for each pretreatment evaluation cycle and a 5 mg/L biocide concentration was maintained in the system throughout all stages to prevent biofouling. Flowrates were kept at 20 mL/min for FS and 600 mL/min for DS in FLS mode and 150 mL/min for both FS and DS in HF mode. Both single- and multiple- cycle evaluations were conducted in this study. A single-cycle evaluation consists of an initial baseline, actual PW fouling test, and a second baseline, while a multiple-cycle evaluation would continue for a second actual PW fouling test and a third baseline. For FLS mode, PRO tests were conducted under the following conditions:

i. Overnight membrane compaction at 20 ± 0.5 bar with DI water on both sides.
ii. Initial baseline for 4 h at 15 ± 0.5 bar with 35 g/L NaCl as FS (mimicking the salinity of SW) and 90–215 g/L NaCl as DS (mimicking the salinity of the PW sample being tested after accounting for dilution losses in the pretreatment stages).
iii. DI water rinse and membrane compaction at 20 ± 0.5 bar overnight with DI water on both sides.
iv. PW fouling test for 4 h at 15 ± 0.5 bar with 35 g/L NaCl FS and pretreated PW as the DS.
v. DI water rinse and membrane compaction (same as #3).
vi. Second baseline (same as #2).
vii. Repeat PW fouling test (same as #4 on a fresh pretreated PW sample).
viii. DI water rinse and membrane compaction (same as #3).
ix. Third baseline (same as #2).

For the HF configuration, membrane pre-stabilization at 10 bar replaced overnight compaction. Actual PW fouling and baseline tests were conducted at only 8 bar to accommodate for the lower membrane pressure tolerance of these HF modules. Both FLS and HF evaluations were carried out for 4 h intervals within practical limits of bench-scale testing. Although longer test duration would provide additional data of the fouling trends, larger PW volumes would be required. At this stage multiple 4 h cycles were used to identify any severe fouling potential based on pretreated water quality and provide an opportunity for comparison of different membrane configurations.

3. Results & discussion

3.1. Pretreatment performance

While limited evaluations of PRO pretreatment requirements have been conducted using actual wastewaters, especially PW from the petroleum industry, in this study three hypersaline PW samples were sourced from selected oil production fields in the United States. Analytical properties of these samples are listed in Table 3. The total dissolved solids (TDS) were calculated as the summation of dissolved ions measured through ion chromatography and ICP. PW 1 and PW 2 had similar salinities but differed considerably in their organic fractions. PW 3 on the other hand, had significantly higher salinity compared to PWs 1 and 2, at this high salinity the TDS to conductivity ratio is above 1 [69]. Out of the three PW samples, PW 1 had the highest TOC (500 mg/ L) while PWs 2 and 3 had comparable TOC values of ≈100 mg/L.

Pretreatment methods were evaluated to maximize removal of

Table 3
Actual PW analytical properties.

Parameter	Unit	PW 1	PW 2	PW 3
pH	–	7.0	7.0	5.0
Conductivity	mS/cm	118	124	252
TDS	mg/L	88,000	93,000	314,000
Turbidity	NTU	290	1100	390
TOC	mg/L	500	120	100
IC	mg/L	24	18	17
TN	mg/L	460	450	2500
Oil & grease	mg/L	480	75	50

organics and suspended solids with %TOC removal used as the main performance metric. 10-micron CF was selected as a baseline for the minimal pretreatment scheme. Different CF sizes were then tested using PW1 (500 mg/L TOC) after coagulation at basic DAF conditions. As shown in Fig. 3, basic DAF treatment achieved 70% TOC removal, this was increased to 78% with post-filtration by 10-micron CF, and to 84% when applying 1-micron CF. Hence, 1-micron CF was selected for the intermediate and extensive pretreatment schemes.

Following definition of the CF size for the various pretreatment levels, three different PAC dosages (250, 500, and 750 mg/L) were tested on PW 1 treated with DAF and 1-micron CF (i.e. TOC of 82 mg/L). The PAC test was followed by 0.45 μm vacuum filtration to separate the treated water from PAC before TOC analysis. Fig. 4 compares the TOC removal for the tested PAC dosages. The control, which consists of only feed PW (PAC dosage of 0 mg/L) showed minimum impact of the testing procedure on the feed TOC (removal <1%). TOC removal stabilized at ≈18% for the two highest dosages and hence 500 mg/L PAC dosage was selected for the extensive pretreatment scheme. While it is understood that PAC might be challenging for application, it was utilized as a traditional organic adsorbent that will be optimized in the future by replacement with more advanced materials.

Basic DAF conditions were developed for a specific water quality reported in literature and involved using a coagulant (120 mg/L $FeCl_3$ as Fe) at a pH of 8.5 and temperature of 25 °C [58]. Since the PW samples used for PRO testing in this study have different characteristics, the effect of using different $FeCl_3$ concentrations on %TOC removal was evaluated. Multiple $FeCl_3$ dosages of 120, 200, 250, and 500 mg/L were evaluated using PW1 as the feed solution and TOC removal results are presented in Fig. 5. Upon increasing the $FeCl_3$ dosage to 200 mg/L, the PW TOC concentration decreased to 58 mg/L. Increasing the coagulant dosage to 250 or 500 mg/L did not result in any further enhancement and 200 mg/L was selected as the optimum $FeCl_3$ dosage.

Table 4 summarizes the analytical results obtained upon applying the various pretreatment schemes on PW 3. Intermediate and minimal pretreatment resulted in final TOC concentrations of 38 and 55 mg/L,
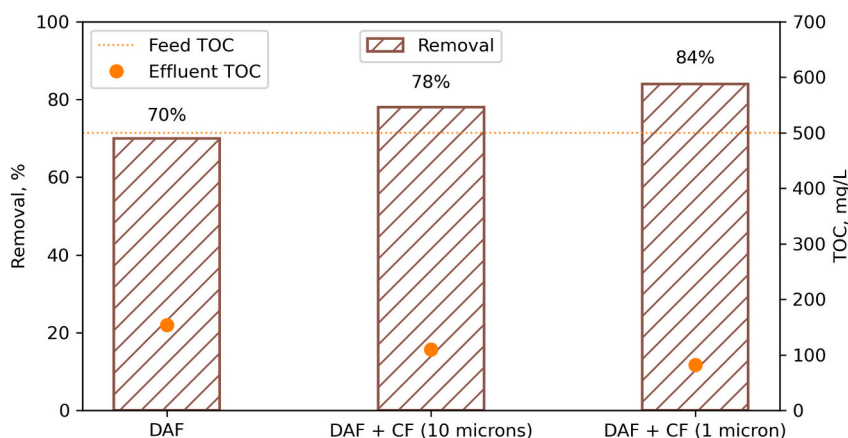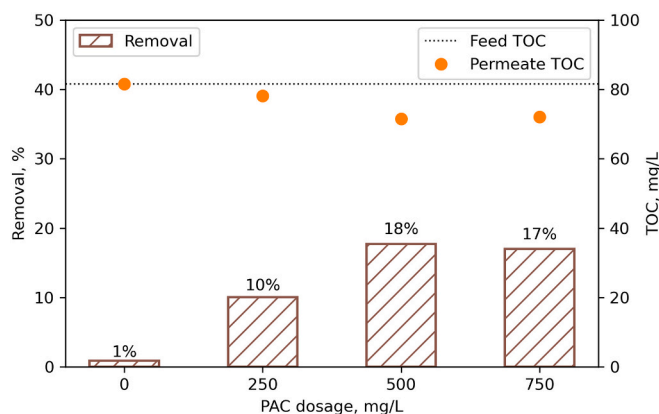
Fig. 4. TOC removal of different PAC dosages (feed water used was PW1 after DAF and 1-micron CF).
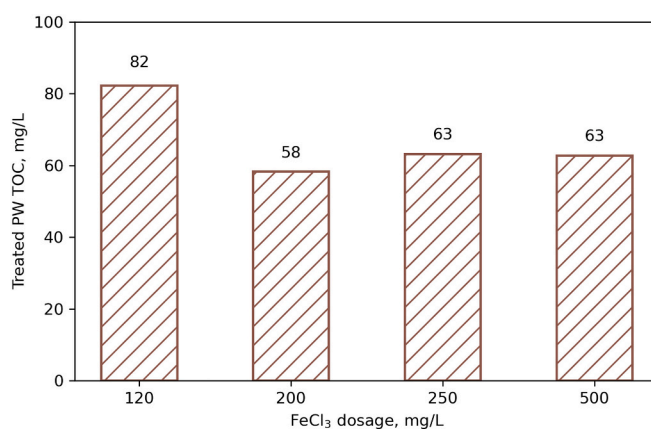
Fig. 5. TOC removal for different $FeCl_3$ dosages (other DAF conditions: 8.5 pH and 25 °C).

respectively. Extensive pretreatment produced a final TOC of 27 mg/L achieving an overall TOC removal of 73%. As for turbidity and TOG, only 87% and 74% removals were achieved by minimal pretreatment respectively while both intermediate and extensive pretreatment schemes resulted in complete turbidity and TOG removals. The drop in conductivity and increase in pH are both attributed to the dilution and pH adjustment during DAF treatment. Table 5 presents a summary of the analytical results for PW1 and PW2 after extensive pretreatment. These pretreated PW samples were then tested in PRO mode to evaluate the

Fig. 3. TOC removal of different CF sizes (basic DAF conditions were used: 120 mg/L $FeCl_3$ as Fe and 8.5 pH followed by 1- or 10-micron CF).

Table 4
Analytical results summary for the applied pretreatment schemes on PW 3.

Parameter	Before pretreatment	After pretreatment			% removals		
		Min.	Inter.	Extn.	Min.	Inter.	Extn.
pH	5.0	5.1	8.5	8.6	–	–	–
Conductivity, mS/cm	252	252	210	207	0%	17%	18%
Turbidity, NTU	390	49	<1	<1	87%	100%	100%
TOC, mg/L	100	55	38	27	45%	62%	73%
TOG, mg/L	50	13	<1	<1	74%	100%	100%

Table 5
Analytical results summary for the extensive pretreatment applied on PW 1 & PW 2.

Parameter	Before pretreatment		After pretreatment		% removal	
	PW 1	PW 2	PW 1	PW 2	PW 1	PW 2
pH	7.0	7.0	8.5	8.5	–	–
Conductivity, mS/cm	118	124	88	82	25%	31%
Turbidity, NTU	290	1100	<1	<1	100%	100%
TOC, mg/L	500	120	48	46	90%	62%
TOG, mg/L	480	75	<1	<1	100%	100%

effectiveness of the different pretreatment schemes in minimizing membrane fouling.

3.2. Membrane performance validation

Three different (Toray TFC FLS) membrane coupons were evaluated to determine their PD at varying operating pressures and validate their performance against predictions of published models [67,68]. Fig. 6 shows the resulting PD of these three coupons and corresponding model predictions. It can be observed that all three coupons produce consistent and reproducible PD data, and the model fitting is in agreement with the experimental values confirming the reliability and accuracy of results. Furthermore, with these FLS coupons applied hydraulic pressures of up to 25 bar are reported enabling representation of the complete PD trend. With increasing applied pressure PD increases reaching a maximum at $\Delta P = \Delta \pi / 2$ and then decreases to 0 when $\Delta P = \Delta \pi$.

A similar evaluation was conducted for the novel HF modules and Fig. 7 shows the resulting PD of one of the membranes tested in duplicate trials. Results indicate consistency and reliability of the data which showed repeatable PD values in multiple trials. These results are also in agreement with previously published evaluations and internal testing conducted by the project team [46]. In contrast to the FLS modules, the complete PD trend is not presented in Fig. 7 due to the limited applied
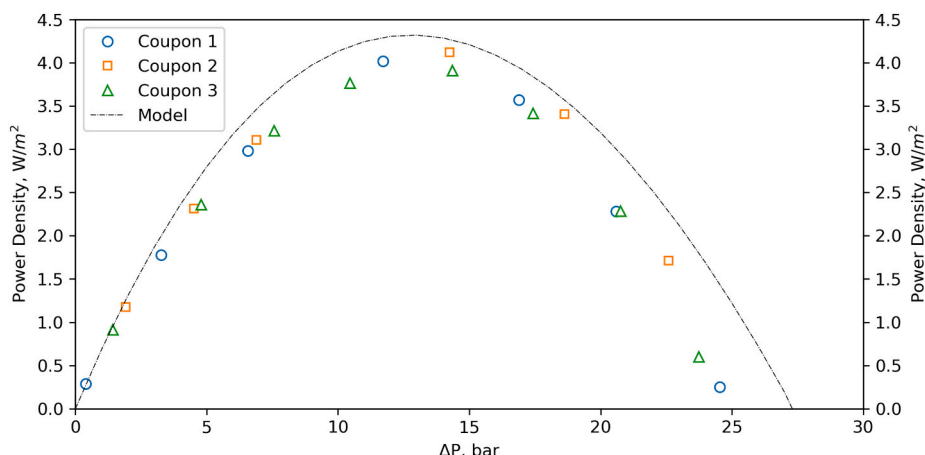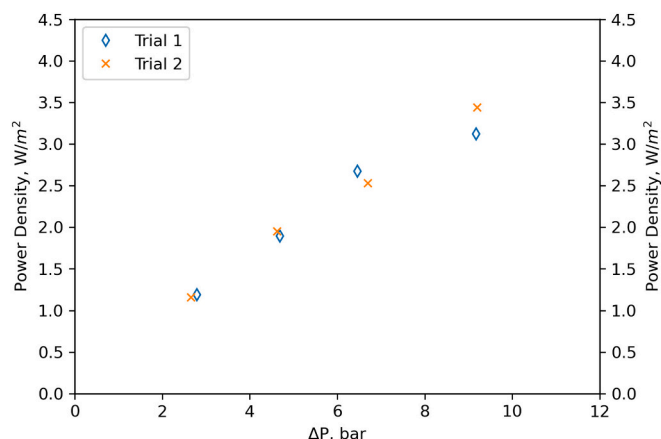

Fig. 7. Power density curve using HF membrane module with 1 M DS at 150 mL/min and DI water FS at 150 mL/min.

pressure tolerance of HF configuration.

3.3. PRO fouling evaluation

Bench scale PRO tests were conducted on the (minimal, intermediate, and extensive) pretreated PW to evaluate the effectiveness of these pretreatment schemes for PRO application and compare fouling behaviors of FLS and HF configurations. The PRO water flux (J_w) using the minimally pretreated PW3 (10-micron CF only) is shown in Fig. 8. The FLS membrane flux at an applied hydraulic pressure of 15 bar is plotted in Fig. 8A. Severe membrane fouling was observed as J_w decreased by 65% from an average of 4.0 LMH in the initial baseline to 1.4 LMH in the final baseline. In contrast, the HF membrane flux (Fig. 8B) remained constant at an average of 12 LMH, under 8 bar applied pressure, for all stages of the experiment. These results suggest lower fouling propensity of HF configuration compared to FLS membranes. However, applied
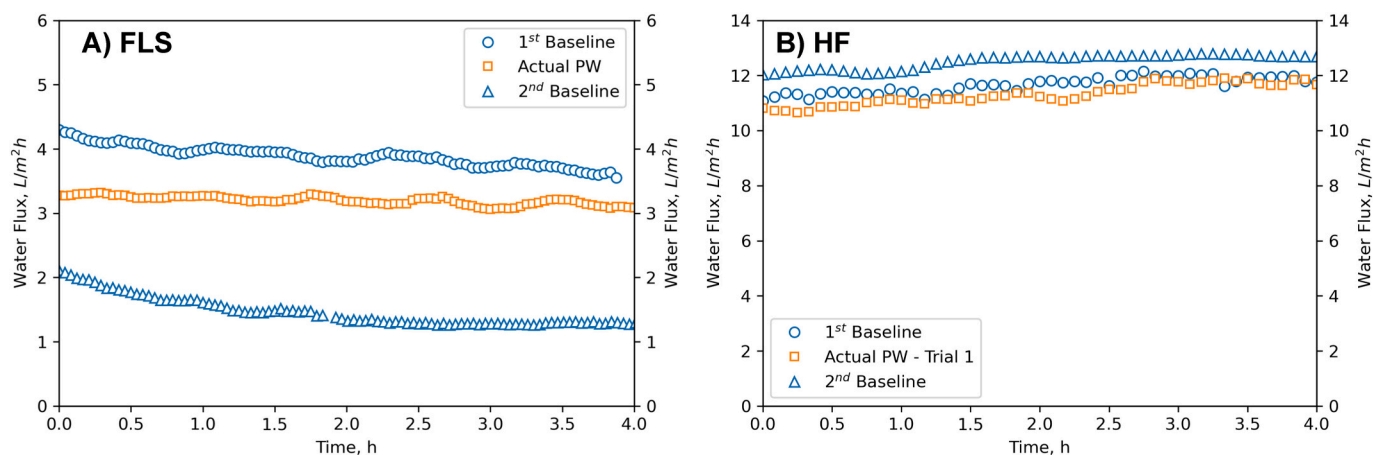

Fig. 6. Power density curve using 3 different Toray FLS membranes with 0.6 M DS at 600 mL/min and DI water FS at 20 mL/min.

Fig. 8. PRO flux for minimal pretreated PW3 or 215 g/L NaCl DS, and 35 g/L NaCl FS.
A) FLS membrane at 15 ± 0.5 bar. B) HF membrane at 8 ± 0.5 bar.

pressure could also be a factor emphasizing the increased fouling in FLS compared to HF PRO experiments. The lower pressure tolerance limit of HF membranes might constitute an obstacle for the application of HF in PRO for energy generation, but lower operating pressures may still be suitable for alternative routes such as PRO for waterflooding.

During PRO operation, the DS salinity was kept constant by dosing 5 M NaCl concentrated stock, however the FS salinity was not fixed to avoid interference in flux measurement (i.e. feed weight reading). Thus, FS salinity increased during the experiment as the FS was concentrated while water passed through to the DS side and salt built up in the FS as a result of reverse salt flux. This decline in effective osmotic driving force resulted in the initial baseline flux of the FLS PRO test (Fig. 8A) decreasing from 4.3 LMH at the beginning of the experiment down to 3.6 LMH at the end of the baseline run. To isolate the effect of FS concentration from the flux loss due to fouling, J_w is normalized by the moving average of the initial baseline flux (J_{w0}) for all stages of the experiment and the resulting plot of normalized flux is shown in Fig. 9A. Due to the lower overall membrane area and better salt rejection of the HF modules less feed concentration effects are observed in the HF test (Fig. 8B). However, for consistency and fair comparisons the normalized flux is also plotted for this experiment in Fig. 9B and all further evaluations. This method of normalization is consistent with published literature studies on membrane fouling as it provides comparative results without affecting overall flux trends [36,42,43,70,71].

The normalized FLS PRO flux (Fig. 9A) decreased from 1 in the first baseline to 0.8 in the PW test and finally down to 0.4 in the final baseline

indicating a 60% reduction in flux due to membrane fouling. In contrast, the normalized PRO flux of the HF membrane test using the same minimally pretreated PW3 showed no decrease throughout all stages of the experiment (Fig. 9B). This normalized result suggests that HF membranes are less prone to fouling compared to FLS coupons in agreement with published literature. Although both the FLS and HF membranes tested are of TFC type, they have different intrinsic membrane properties (Table 2). These different properties could affect the fouling propensity of the tested membranes and contribute to their varying behavior. The hydrodynamics of the HF and FLS membrane modules also play a role in their fouling potential. The HF membranes, due to their configuration, could withstand higher cross flow velocities compared to FLS since they are self-supported, which eliminates the need of spacers [72,73]. This improvement in the hydrodynamics enhances the shear forces on the membrane surface reducing fouling deposits [74].

Next, the effectiveness of intermediate pretreatment (DAF and 1-micron CF) for PW3 as DS was evaluated in both FLS and HF PRO tests. Fig. 10 shows the resulting normalized PRO water flux. All baseline runs exhibited a normalized flux of ~1 indicating no fouling for both membrane configurations tested. These results suggest that intermediate pretreatment is sufficient for both FLS and HF configurations under the presented bench-scale conditions.

Extensively pretreated (DAF, 1-micron CF, PAC, and MF) PW3 and PW2 samples were tested as DS for PRO in FLS configuration. This was not required for the HF configuration since both minimal and
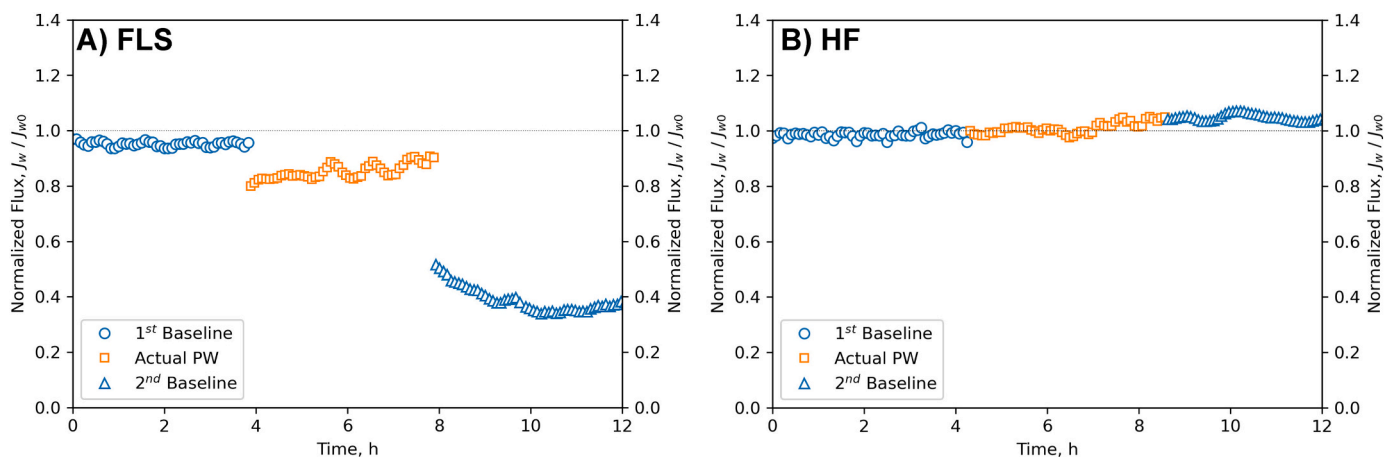

Fig. 9. Normalized PRO water flux for minimal pretreated PW3 or 215 g/L NaCl DS, and 35 g/L NaCl FS.
A) FLS membrane at 15 ± 0.5 bar and J_{w0} ~4.0 LMH. B) HF membrane at 8 ± 0.5 bar and J_{w0} ~12 LMH.

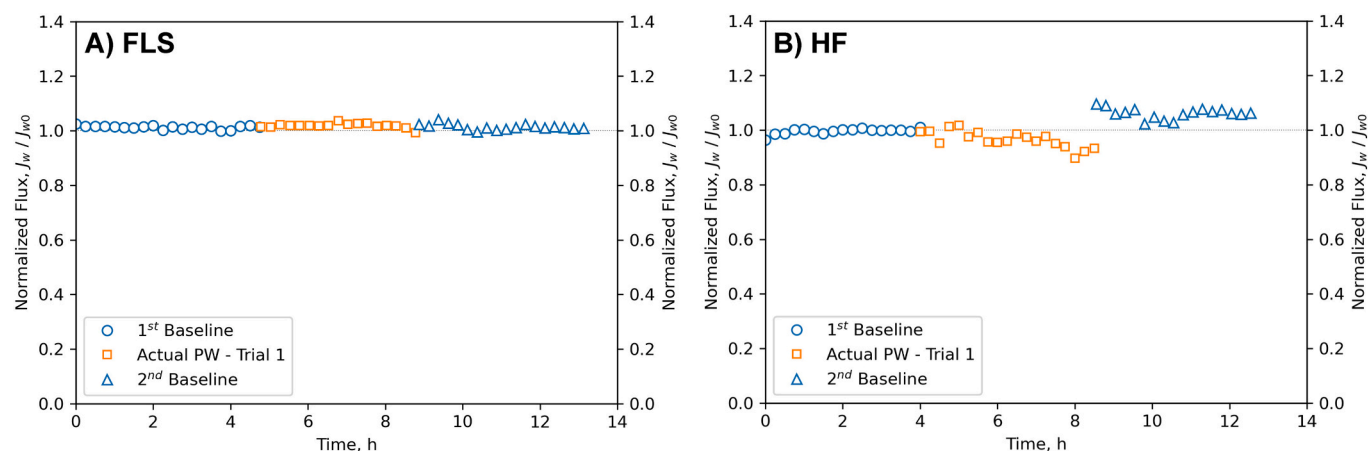**Fig. 10.** Normalized PRO water flux for intermediate pretreated PW3 or 215 g/L NaCl DS, and 35 g/L NaCl FS.
A. FLS membrane at 14 ± 0.5 bar and $J_{w0} \sim 4.2$ LMH. B) HF membrane at 8 ± 0.5 bar and $J_{w0} \sim 10.0$ LMH.

intermediate pretreatment evaluations using the HF membranes did not show any fouling. Fig. 11A and B shows the resulting normalized PRO flux for PW3 and PW2 respectively. Less than 1% decline in flux was observed throughout all stages of the experiment confirming no fouling effects on the membranes.

The water flux data of single-cycle evaluations indicates that PW can be treated to suitable levels for PRO application to avoid membrane fouling. These fit-for-purpose pretreatment schemes enable removal of organics and suspended solids present in PW to acceptable levels for the PRO process. The power density for the PW evaluations was calculated based on average PRO flux under non-fouling conditions at the specified pressure for both membranes. Approximately, 2 W/m^2 is estimated for the FLS coupons and 3 W/m^2 for the HF modules. These values can be significantly increased through the development of membranes that are more resistant to internal concentration polarization effects and would enable harnessing the actual osmotic potential of this solution pairing. The team later evaluated multiple PRO fouling cycles to ensure consistency and reproducibility of the data and assess any impact additional cycles would have on the membrane performance. For this multiple cycle evaluation, extensive pretreatment was used for FLS tests and minimal pretreatment for the HF tests. Fig. 12A shows the resulting normalized PRO flux when using extensive pretreated PW3 as DS for FLS operation. The normalized flux remained at ~1 over the multiple-cycle evaluation confirming no membrane fouling occurred. Similarly, Fig. 12B shows the PRO water flux for the HF test with minimally

pretreated PW3 as DS. Again, less than 1% decline in flux is observed over the entire experiment duration confirming the previous single-cycle evaluation results.

Based on these bench scale results; minimal pretreatment of PW seems to be sufficient for HF PRO applications while intermediate pretreatment could also be applied in case a more conservative approach is recommended. In contrast, using FLS membranes in PRO application requires applying at least intermediate to extensive levels of PW pretreatment to avoid severe membrane fouling. Validation of these results and optimization of the pretreatment technologies requires long term pilot testing. The cost implications of applying these advanced treatment technologies must also be considered through detailed techno-economic analyses.

To validate the fouling performance obtained in PRO bench scale evaluation of the Toray FLS membranes tested, FTIR analysis was performed on clean and fouled membrane samples after oven drying at 105 °C. This analysis enables identification and comparison of key functional groups from the compounds deposited on the membranes. Fig. 13A compares the FTIR spectra in transmittance% against wavelength (500–4000 cm^{-1}) for a clean Toray FLS coupon against the PRO tested coupons using pretreated PW3 at the minimal, intermediate, and extensive levels. Peaks corresponding to C—H stretching vibrations at wavelengths of 2966 and 2922 cm^{-1} were observed on all membrane samples [75,76]. Upon analyzing the membrane tested using minimally pretreated PW, it was noticed that those two C—H peaks are intensified
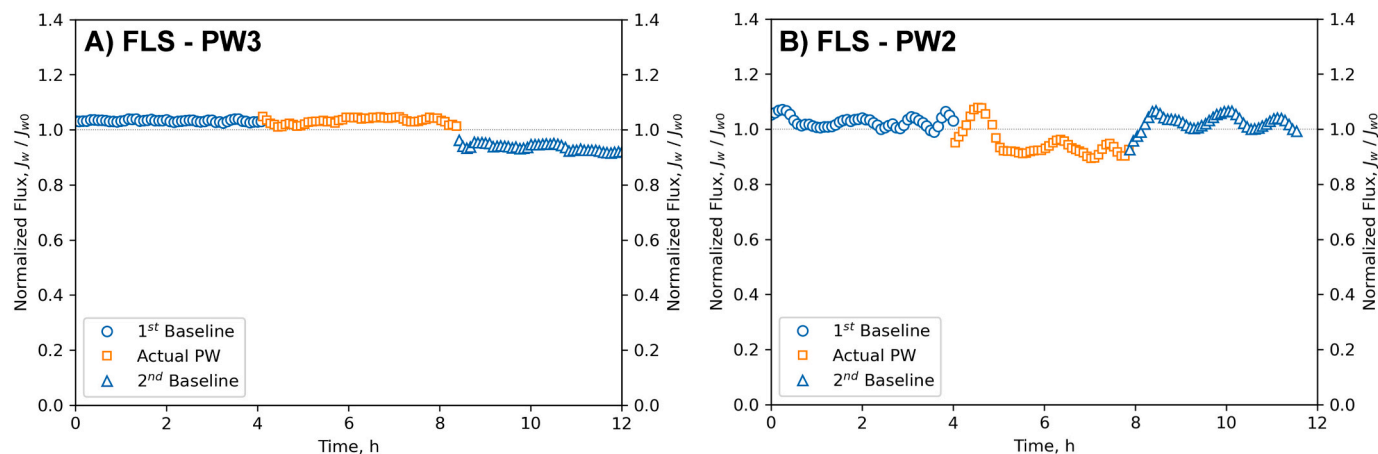

Fig. 11. Normalized PRO water flux for FLS membranes and 35 g/L NaCl FS at 15 ± 0.5 bar.
A) Extensively pretreated PW3 or 215 g/L NaCl DS and J_{w0} of 7.0 LMH.
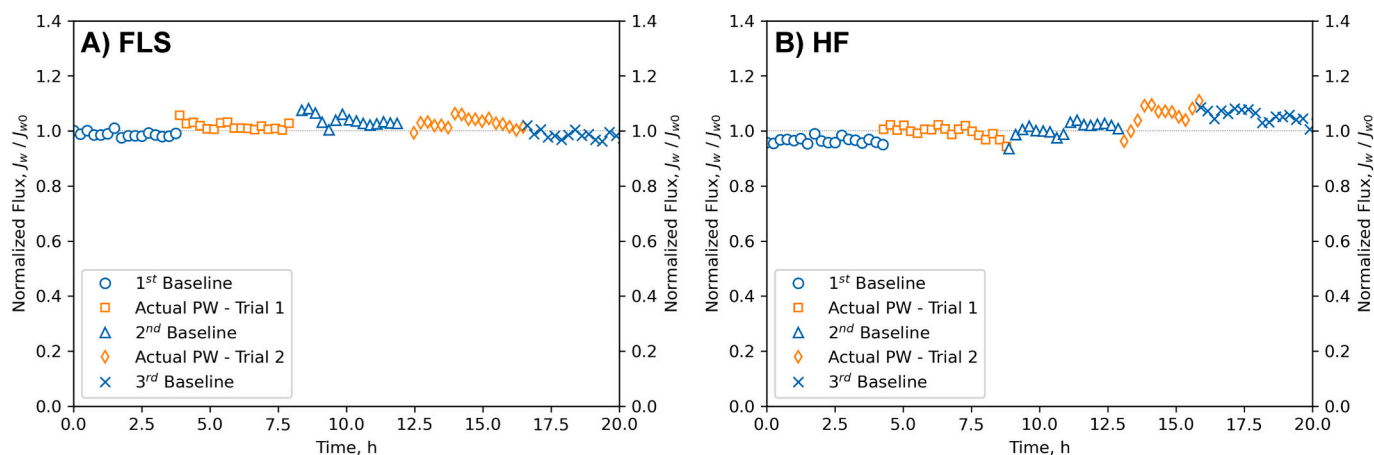B) Extensively pretreated PW2 or 93 g/L NaCl DS and J_{w0} of 3.1 LMH.

Fig. 12. Multiple cycle evaluations of PRO flux. FLS first.
A) FLS membrane, extensive pretreated PW3 at 15 ± 0.5 bar ($J_{w0} \sim 4.3$ LMH).
B) HF membrane, minimal pretreated PW3 at 8 ± 0.5 bar ($J_{w0} \sim 10.3$ LMH).

suggesting that more organics were deposited on the membrane after this PRO fouling test. These results are also supported by images taken for each of the tested membranes as indicated in Fig. 13B. The membrane surface image at minimal pretreatment confirms the deposition of contaminants from the PW and resulting flux decline detected in the PRO test. On the contrary, the FTIR spectra for both intermediate and extensive pretreatment levels were found to be comparable to the clean membrane coupon. In addition, the surface images taken at those pretreatment levels did not show any clear deposition of contaminants as compared to the minimal level which again validates obtained PRO bench scale results. Enhanced O—H stretching vibration at a wavelength of 3304 cm^{-1} was noticed only at the minimal level indicating the deposition of some carboxylic acids that are not removed at the minimal treatment level and possibly attributing to membrane fouling [77].

3.4. PRO economics and potential application

As in most membrane applications, feed pretreatment is critical and PRO is no exception. Membrane treatment of PW, with its added chemicals, poses particular challenges. The test results show that rigorous pretreatment, including DAF and post filtration, is required to prevent rapid fouling of the membranes. While this pretreatment will be comparatively expensive, it has to be taken in context with the value of the "product" of the PRO process. When PRO is applied to produce or save electrical energy, the annual economic benefit is <$500 per module and the process is not considered economically feasible [33]. When PRO is applied for waterflooding, the product is oil, not energy, and the economic benefit is projected to be >$70,000/yr for an 8″ spiral wound module [33]. At this level of economic benefit, even with extensive pretreatment, the economics are expected to be favorable.

While this study is a proof-of-concept to identify possible pretreatment strategies and evaluate innovative membrane products, further assessment and optimization of pretreatment options needs to be done via long-term pilot testing under relevant field conditions. More emphasis must also be given to the production of enhanced PRO membranes that are more resistant to fouling and concentration polarization effects. This will generate the needed data to further validate process feasibility and identify fit-for-purpose applications.

4. Summary & conclusions

This study focused on comparing various levels of PW pretreatment for PRO application and evaluated the effect of membrane configuration on PRO fouling rates. Actual hypersaline PW samples were sourced from selected oil production fields in the United States. The PWs were first

characterized and then pretreated to varying degrees by a combination of physical and/or physicochemical processes targeting the removal of organics and suspended solids. Salinities of these PWs ranged between 90 and 300 g/L while TOCs were at 100–500 mg/L. The effectiveness of pretreatment technologies was then compared in PRO bench scale tests using both FLS membranes and novel HF modules. To the authors' knowledge this evaluation is the first to use actual PW for PRO application, develop appropriate pretreatment strategies, and compare fouling propensity of different PRO membrane configurations. Main conclusions of this evaluation include:

1. The PRO bench scale system generated reproducible and reliable PD data compared to published process models.
2. FLS testing enabled operation at a high-pressure range producing the full PD trend, in contrast HF modules had limited applied pressure tolerance which constricted generation of a similar plot.
3. Minimal pretreatment reduced the turbidity and TOC of PW3 by 87% and 45% respectively, while extensive pretreatment enhanced those removals to 100% for turbidity and 73% for TOC.
4. HF membranes showed less fouling propensity than FLS coupons during the PRO test with minimally pretreated PW; where <1% flux decline was observed for HF compared to 60% decrease in FLS water flux.
5. Both minimal and intermediate levels of pretreatment were sufficient for the HF configuration and resulted in <1% decrease of PRO flux.
6. Intermediate and extensive levels of pretreatment were required to maintain PRO flux in FLS mode with <1% decline.
7. Multiple PRO fouling cycles provided insight into the stability of the flux and ensured consistency of the data confirming initial single-cycle observations.

These results verify that PW can be treated to suitable levels for PRO application without entailing severe membrane fouling given sufficient pretreatment is applied. It is noted that, even with advanced pretreatment, PRO economics still appear to be favorable when applied for waterflooding operations in O&G operations. Further studies should focus on developing an optimal combination of the most cost-effective pretreatment technologies, fabricating more foulant resistant membranes that are not susceptible to concentration polarization effects, evaluating membrane cleaning protocols, and conducting long-term pilot testing with detailed techno-economic assessments for further process validation and optimization.
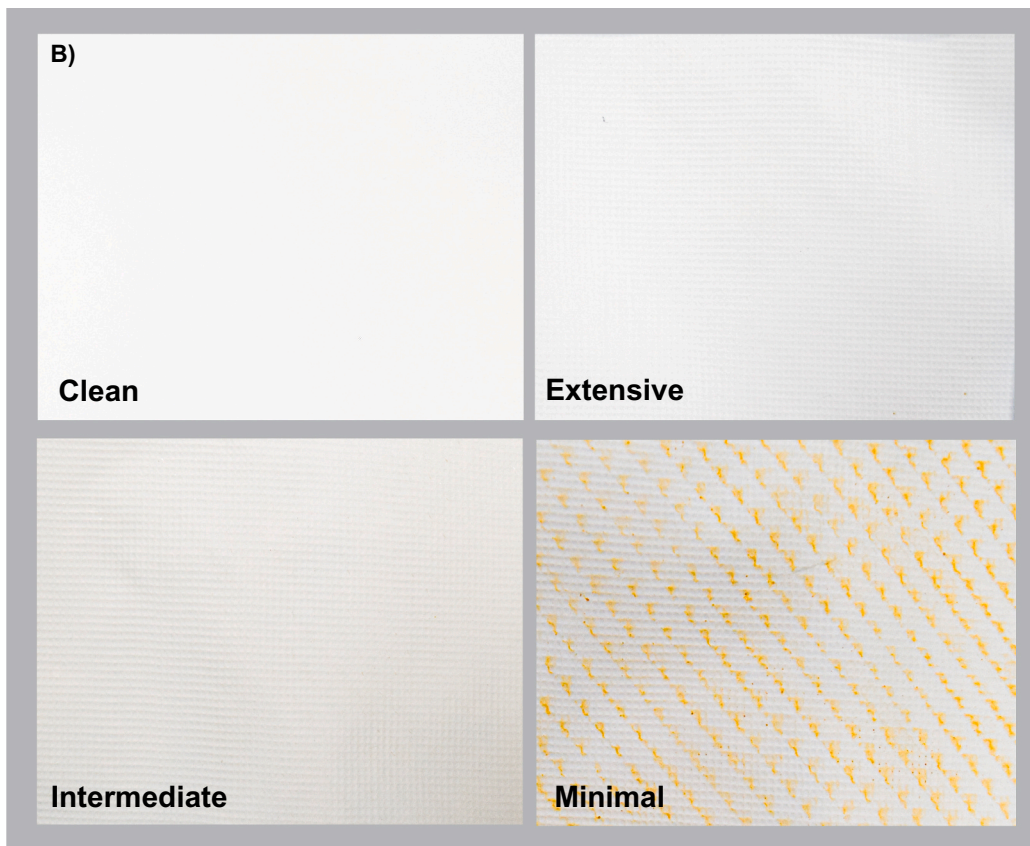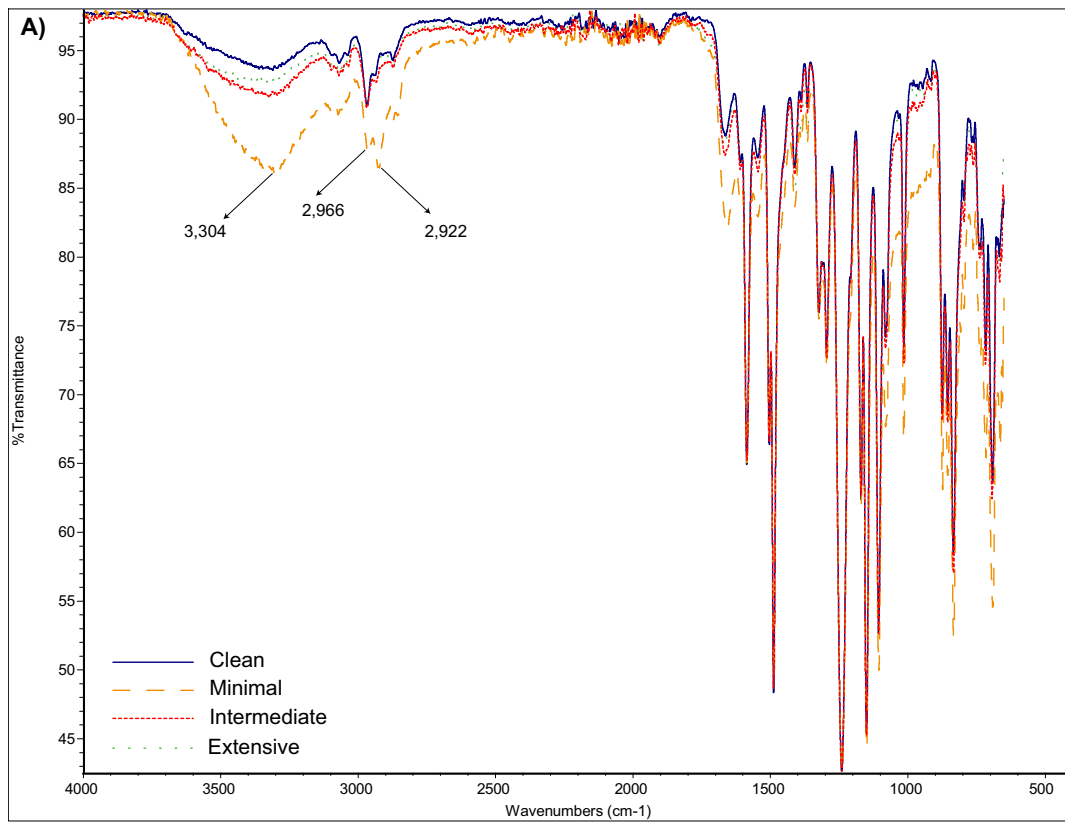
Fig. 13. A) FTIR spectra for clean and fouled Toray FLS membranes. B) Surface images for clean and fouled Toray FLS membranes.

CRediT authorship contribution statement

Dareen Dardor: Methodology, Formal analysis, Investigation, Writing – Original draft
Mashael Al Maas: Data curation, Validation
Joel Minier-Matar: Software, Visualization
Arnold Janson: Writing – Review & editing
Ahmed Abdel-Wahab: Supervision
Ho Kyong Shon: Supervision
Samer Adham: Conceptualization, Supervision, Funding acquisition.

Declaration of competing interest

The authors declare that they have no known competing financial interests or personal relationships that could have appeared to influence the work reported in this paper.

References

[1] M.I. Hoffert, K. Caldeira, G. Benford, D.R. Criswell, C. Green, H. Herzog, A.K. Jain, H.S. Kheshgi, K.S. Lackner, J.S. Lewis, H.D. Lightfoot, W. Manheimer, J.C. Mankins, M.E. Mauel, L.J. Perkins, M.E. Schlesinger, T. Volk, T.M.L. Wigley, Advanced technology paths to global climate stability: energy for a greenhouse planet, Science (80-.) 298 (2002) 981 LP–987 LP, https://doi.org/10.1126/science.1072357.

[2] R.L. McGinnis, M. Elimelech, Global challenges in energy and water supply: the promise of engineered osmosis, Environ. Sci. Technol. 42 (2008) 8625–8629, https://doi.org/10.1021/es800812m.

[3] R.E. Pattle, Production of electric power by mixing fresh and salt water in the hydroelectric pile, Nature 174 (1954) 660, https://doi.org/10.1038/174660a0.

[4] J.W. Post, J. Veerman, H.V.M. Hamelers, G.J.W. Euverink, S.J. Metz, K. Nymeijer, C.J.N. Buisman, Salinity-gradient power: evaluation of pressure-retarded osmosis and reverse electrodialysis, J. Memb. Sci. 288 (2007) 218–230, https://doi.org/10.1016/j.memsci.2006.11.018.

[5] B.E. Logan, M. Elimelech, Membrane-based processes for sustainable power generation using water, Nature 488 (2012) 313–319, https://doi.org/10.1038/nature11477.

[6] T. Thorsen, T. Holt, The potential for power production from salinity gradients by pressure retarded osmosis, J. Memb. Sci. 335 (2009) 103–110, https://doi.org/10.1016/j.memsci.2009.03.003.

[7] N.Y. Yip, M. Elimelech, Thermodynamic and energy efficiency analysis of power generation from natural salinity gradients by pressure retarded osmosis, Environ. Sci. Technol. 46 (2012) 5230–5239, https://doi.org/10.1021/es300060m.

[8] N.Y. Yip, D.A. Vermaas, K. Nijmeijer, M. Elimelech, Environ. Sci. Technol. 48 (2014) 4925–4936, https://doi.org/10.1021/es5005413.

[9] D.A. Vermaas, J. Veerman, N.Y. Yip, M. Elimelech, M. Saakes, K. Nijmeijer, High efficiency in energy generation from salinity gradients with reverse electrodialysis, ACS Sustain. Chem. Eng. 1 (2013) 1295–1302, https://doi.org/10.1021/sc400150w.

[10] N.Y. Yip, D. Brogioli, H.V.M. Hamelers, K. Nijmeijer, Salinity gradients for sustainable energy: primer, progress, and prospects, Environ. Sci. Technol. 50 (2016) 12072–12094, https://doi.org/10.1021/acs.est.6b03448.

[11] M.C. Hatzell, R.D. Cusick, B.E. Logan, Capacitive mixing power production from salinity gradient energy enhanced through exoelectrogen-generated ionic currents, Energy Environ. Sci. 7 (2014) 1159–1165, https://doi.org/10.1039/C3EE43823F.

[12] N.Y. Yip, M. Elimelech, Comparison of energy efficiency and power density in pressure retarded osmosis and reverse electrodialysis, Environ. Sci. Technol. 48 (2014) 11002–11012, https://doi.org/10.1021/es5029316.

[13] S. Loeb, R.S. Norman, Osmotic power plants, Science (80-.) 189 (1975) 654 LP–655 LP, https://doi.org/10.1126/science.189.4203.654.

[14] A. Achilli, A.E. Childress, Pressure retarded osmosis: from the vision of Sidney Loeb to the first prototype installation — review, Desalination 261 (2010) 205–211, https://doi.org/10.1016/j.desal.2010.06.017.

[15] R.R. Gonzales, A. Abdel-Wahab, S. Adham, D.S. Han, S. Phuntsho, W. Suwaileh, N. Hilal, H.K. Shon, Salinity gradient energy generation by pressure retarded osmosis: a review, Desalination 500 (2021) 114841, https://doi.org/10.1016/j.desal.2020.114841.

[16] H. Manzoor, M.A. Selam, S. Adham, H.K. Shon, M. Castier, A. Abdel-Wahab, Energy recovery modeling of pressure-retarded osmosis systems with membrane modules compatible with high salinity draw streams, Desalination 493 (2020) 114624, https://doi.org/10.1016/j.desal.2020.114624.

[17] S.L. Plata, A.E. Childress, Limiting power density in pressure-retarded osmosis: observation and implications, Desalination 467 (2019) 51–56, https://doi.org/10.1016/j.desal.2019.05.013.

[18] B. Blankert, Y. Kim, H. Vrouwenvelder, N. Ghaffour, Facultative hybrid RO-PRO concept to improve economic performance of PRO: feasibility and maximizing efficiency, Desalination 478 (2020) 114268, https://doi.org/10.1016/j.desal.2019.114268.

[19] S. Sarp, N. Hilal, Thermodynamic optimization of Multistage pressure Retarded Osmosis (MPRO) with variable feed pressures for hypersaline solutions, Desalination 477 (2020) 114245, https://doi.org/10.1016/j.desal.2019.114245.

[20] A. Altaee, N. Hilal, Dual-stage forward osmosis/pressure retarded osmosis process for hypersaline solutions and fracking wastewater treatment, Desalination 350 (2014) 79–85, https://doi.org/10.1016/j.desal.2014.07.013.

[21] Statkraft, Crown Princess to Open World's First osmotic power plant, Press Release, Oslo, Norw, 2009. https://www.statkraft.cl/en/noticias2/press-releases/Press-releases-archive/2009/crown-princess-mette-marit-to-open-the-worlds-first-osmotic-power-plant/.

[22] A. Tanioka, Preface to the special issue on "pressure retarded osmosis in megaton water system project", Desalination 389 (2016) 15–17, https://doi.org/10.1016/j.desal.2016.02.013.

[23] H. Sakai, T. Ueyama, M. Irie, K. Matsuyama, A. Tanioka, K. Saito, A. Kumano, Energy recovery by PRO in sea water desalination plant, Desalination 389 (2016) 52–57, https://doi.org/10.1016/j.desal.2016.01.025.

[24] S. Lee, J. Choi, Y.-G. Park, H. Shon, C.H. Ahn, S.-H. Kim, Hybrid desalination processes for beneficial use of reverse osmosis brine: current status and future prospects, Desalination 454 (2019) 104–111, https://doi.org/10.1016/j.desal.2018.02.002.

[25] E. Drioli, Membrane Distillation, MDPI AG, 2018. https://books.google.com.qa/books?id=as1SDwAAQBAJ.

[26] Z.M. Binger, G. O'Toole, A. Achilli, Evidence of solution-diffusion-with-defects in an engineering-scale pressure retarded osmosis system, J. Memb. Sci. 625 (2021), 119135, https://doi.org/10.1016/j.memsci.2021.119135.

[27] A.P. Straub, A. Deshmukh, M. Elimelech, Pressure-retarded osmosis for power generation from salinity gradients: is it viable? Energy Environ. Sci. 9 (2016) 31–48, https://doi.org/10.1039/C5EE02985F.

[28] Y.C. Kim, M. Elimelech, Potential of osmotic power generation by pressure retarded osmosis using seawater as feed solution: analysis and experiments, J. Memb. Sci. 429 (2013) 330–337, https://doi.org/10.1016/j.memsci.2012.11.039.

[29] S. Adham, A. Hussain, J. Minier-Matar, A. Janson, R. Sharma, Membrane applications and opportunities for water management in the oil & gas industry, Desalination 440 (2018) 2–17, https://doi.org/10.1016/j.desal.2018.01.030.

[30] J. Veil, C. Clark, Produced water volume estimates and management practices, SPE Prod. Oper. 26 (2011) 234–239, https://doi.org/10.2118/125999-PA.

[31] E. Emam, T.M. Moawad, N. Aboul-Gheit, Evaluating the characteristics of offshore oilfield produced water, Pet. Coal. 56 (2014) 363–372.

[32] L. Li, Q. Qu, H. Sun, J. Zhou, M. Legemah, How extremely high-TDS produced water compositions affect selection of fracturing fluid additives, SPE Int. Symp. Oilf. Chem. (2015) 17, https://doi.org/10.2118/173746-MS.

[33] A. Janson, D. Dardor, M. Al Maas, J. Minier-Matar, A. Abdel-Wahab, S. Adham, Pressure-retarded osmosis for enhanced oil recovery, Desalination 491 (2020) 114568, https://doi.org/10.1016/j.desal.2020.114568.

[34] Number 8 T. Pankratz, Global Water Intelligence, Water Desalination Report 57, 2021.

[35] J. Kim, M.J. Park, M. Park, H.K. Shon, S.-H. Kim, J.H. Kim, Influence of colloidal fouling on pressure retarded osmosis, Desalination 389 (2016) 207–214, https://doi.org/10.1016/j.desal.2016.01.036.

[36] E. Bar-Zeev, F. Perreault, A.P. Straub, M. Elimelech, Impaired performance of pressure-retarded osmosis due to irreversible biofouling, Environ. Sci. Technol. 49 (2015) 13050–13058, https://doi.org/10.1021/acs.est.5b03523.

[37] T. Yang, C.F. Wan, J.Y. Xiong, T.-S. Chung, Pre-treatment of wastewater retentate to mitigate fouling on the pressure retarded osmosis (PRO) process, Sep. Purif. Technol. 215 (2019) 390–397, https://doi.org/10.1016/j.seppur.2019.01.032.

[38] C.F. Wan, S. Jin, T.-S. Chung, Mitigation of inorganic fouling on pressure retarded osmosis (PRO) membranes by coagulation pretreatment of the wastewater concentrate feed, J. Memb. Sci. 572 (2019) 658–667, https://doi.org/10.1016/j.memsci.2018.11.051.

[39] Q. She, L. Zhang, R. Wang, W.B. Krantz, A.G. Fane, Pressure-retarded osmosis with wastewater concentrate feed: fouling process considerations, J. Memb. Sci. 542 (2017) 233–244, https://doi.org/10.1016/j.memsci.2017.08.022.

[40] G. Han, J. Zhou, C. Wan, T. Yang, T.-S. Chung, Investigations of inorganic and organic fouling behaviors, antifouling and cleaning strategies for pressure retarded osmosis (PRO) membrane using seawater desalination brine and wastewater, Water Res. 103 (2016) 264–275, https://doi.org/10.1016/j.watres.2016.07.040.

[41] L. Zhang, Q. She, R. Wang, S. Wongchitphimon, Y. Chen, A.G. Fane, Unique roles of aminosilane in developing anti-fouling thin film composite (TFC) membranes for pressure retarded osmosis (PRO), Desalination 389 (2016) 119–128, https://doi.org/10.1016/j.desal.2015.12.024.

[42] J. Ju, Y. Choi, S. Lee, Y.-G. Park, Comparison of different pretreatment methods for pressure retarded osmosis (PRO) membrane in bench-scale and pilot-scale systems, Desalination 496 (2020) 114528, https://doi.org/10.1016/j.desal.2020.114528.

[43] N.Y. Yip, M. Elimelech, Environ. Sci. Technol. 47 (2013) 12607–12616, https://doi.org/10.1021/es403207m.

[44] R.R. Gonzales, M.J. Park, T.-H. Bae, Y. Yang, A. Abdel-Wahab, S. Phuntsho, H. K. Shon, Melamine-based covalent organic framework-incorporated thin film nanocomposite membrane for enhanced osmotic power generation, Desalination 459 (2019) 10–19, https://doi.org/10.1016/j.desal.2019.02.013.

[45] Q. She, J. Wei, N. Ma, V. Sim, A.G. Fane, R. Wang, C.Y. Tang, Fabrication and characterization of fabric-reinforced pressure retarded osmosis membranes for osmotic power harvesting, J. Memb. Sci. 504 (2016) 75–88, https://doi.org/10.1016/j.memsci.2016.01.004.

[46] M.J. Park, S. Lim, R.R. Gonzales, S. Phuntsho, D.S. Han, A. Abdel-Wahab, S. Adham, H.K. Shon, Thin-film composite hollow fiber membranes incorporated with graphene oxide in polyethersulfone support layers for enhanced osmotic power density, Desalination 464 (2019) 63–75, https://doi.org/10.1016/j.desal.2019.04.026.

[47] S. Chou, R. Wang, L. Shi, Q. She, C. Tang, A.G. Fane, Thin-film composite hollow fiber membranes for pressure retarded osmosis (PRO) process with high power density, J. Memb. Sci. 389 (2012) 25–33, https://doi.org/10.1016/j.memsci.2011.10.002.

[48] S. Chou, L. Shi, R. Wang, C.Y. Tang, C. Qiu, A.G. Fane, Characteristics and potential applications of a novel forward osmosis hollow fiber membrane, Desalination 261 (2010) 365–372, https://doi.org/10.1016/j.desal.2010.06.027.

[49] B.D. Coday, P. Xu, E.G. Beaudry, J. Herron, K. Lampi, N.T. Hancock, T.Y. Cath, The sweet spot of forward osmosis: treatment of produced water, drilling wastewater, and other complex and difficult liquid streams, Desalination 333 (2014) 23–35, https://doi.org/10.1016/j.desal.2013.11.014.

[50] E. Sivertsen, T. Holt, W. Thelin, G. Brekke, Pressure retarded osmosis efficiency for different hollow fibre membrane module flow configurations, Desalination 312 (2013) 107–123, https://doi.org/10.1016/j.desal.2012.11.019.

[51] M. Shibuya, M. Yasukawa, T. Takahashi, T. Miyoshi, M. Higa, H. Matsuyama, Effects of operating conditions and membrane structures on the performance of hollow fibre forward osmosis membranes in pressure assisted osmosis, Desalination 365 (2015) 381–388, https://doi.org/10.1016/j.desal.2015.03.005.

[52] K.J. Howe, A. Marwah, K.-P. Chiu, S.S. Adham, Effect of membrane configuration on bench-scale MF and UF fouling experiments, Water Res. 41 (2007) 3842–3849, https://doi.org/10.1016/j.watres.2007.05.025.

[53] J. Minier-Matar, A. Santos, A. Hussain, A. Janson, R. Wang, A.G. Fane, S. Adham, Application of hollow fiber forward osmosis membranes for produced and process water volume reduction: an osmotic concentration process, Environ. Sci. Technol. 50 (2016) 6044–6052, https://doi.org/10.1021/acs.est.5b04801.

[54] D.A. Ladner, A. Subramani, M. Kumar, S.S. Adham, M.M. Clark, Bench-scale evaluation of seawater desalination by reverse osmosis, Desalination 250 (2010) 490–499, https://doi.org/10.1016/j.desal.2009.06.072.

[55] G. Amy, N. Ghaffour, Z. Li, L. Francis, R.V. Linares, T. Missimer, S. Lattemann, Membrane-based seawater desalination: present and future prospects, Desalination 401 (2017) 16–21, https://doi.org/10.1016/j.desal.2016.10.002.

[56] P. Zhang, P. Knötig, S. Gray, M. Duke, Scale reduction and cleaning techniques during direct contact membrane distillation of seawater reverse osmosis brine, Desalination 374 (2015) 20–30, https://doi.org/10.1016/j.desal.2015.07.005.

[57] J. Zhang, K. Northcott, M. Duke, P. Scales, S.R. Gray, Influence of pre-treatment combinations on RO membrane fouling, Desalination 393 (2016) 120–126, https://doi.org/10.1016/j.desal.2016.02.020.

[58] M. Nadella, R. Sharma, S. Chellam, Fit-for-purpose treatment of produced water with iron and polymeric coagulant for reuse in hydraulic fracturing: temperature effects on aggregation and high-rate sedimentation, Water Res. 170 (2020) 115330, https://doi.org/10.1016/j.watres.2019.115330.

[59] A.P. Straub, N.Y. Yip, M. Elimelech, Raising the bar: increased hydraulic pressure allows unprecedented high power densities in pressure-retarded osmosis, Environ. Sci. Technol. Lett. 1 (2014) 55–59, https://doi.org/10.1021/ez400117d.

[60] Z.L. Cheng, X. Li, Y. Feng, C.F. Wan, T.-S. Chung, Tuning water content in polymer dopes to boost the performance of outer-selective thin-film composite (TFC) hollow fiber membranes for osmotic power generation, J. Memb. Sci. 524 (2017) 97–107, https://doi.org/10.1016/j.memsci.2016.11.009.

[61] W. Gai, X. Li, J.Y. Xiong, C.F. Wan, T.-S. Chung, Evolution of micro-deformation in inner-selective thin film composite hollow fiber membranes and its implications for osmotic power generation, J. Memb. Sci. 516 (2016) 104–112, https://doi.org/10.1016/j.memsci.2016.06.007.

[62] S. Chou, R. Wang, A.G. Fane, Robust and High performance hollow fiber membranes for energy harvesting from salinity gradients by pressure retarded osmosis, J. Memb. Sci. 448 (2013) 44–54, https://doi.org/10.1016/j.memsci.2013.07.063.

[63] M. Son, H. Park, L. Liu, H. Choi, J.H. Kim, H. Choi, Thin-film nanocomposite membrane with CNT positioning in support layer for energy harvesting from saline water, Chem. Eng. J. 284 (2016) 68–77, https://doi.org/10.1016/j.cej.2015.08.134.

[64] S. Zhang, F. Fu, T.-S. Chung, Substrate modifications and alcohol treatment on thin film composite membranes for osmotic power, Chem. Eng. Sci. 87 (2013) 40–50, https://doi.org/10.1016/j.ces.2012.09.014.

[65] G. Han, S. Zhang, X. Li, T.-S. Chung, High performance thin film composite pressure retarded osmosis (PRO) membranes for renewable salinity-gradient energy generation, J. Memb. Sci. 440 (2013) 108–121, https://doi.org/10.1016/j.memsci.2013.04.001.

[66] J.A. Idarraga-Mora, D.A. Ladner, S.M. Husson, Thin-film composite membranes on polyester woven mesh with variable opening size for pressure-retarded osmosis, J. Memb. Sci. 549 (2018) 251–259, https://doi.org/10.1016/j.memsci.2017.12.023.

[67] J. Benjamin, M.E. Arias, Q. Zhang, A techno-economic process model for pressure retarded osmosis based energy recovery in desalination plants, Desalination 476 (2020), 114218, https://doi.org/10.1016/j.desal.2019.114218.

[68] H. Manzoor, M.A. Selam, F.Bin Abdur Rahman, S. Adham, M. Castier, A. Abdel-Wahab, A tool for assessing the scalability of pressure-retarded osmosis (PRO) membranes, Renew. Energy 149 (2020) 987–999, https://doi.org/10.1016/j.renene.2019.10.098.

[69] L.R.B. Rebello, T. Siepman, S. Drexler, Correlations between TDS and electrical conductivity for high-salinity formation brines characteristic of South Atlantic pre-salt basins, Water SA 46 (2020), https://doi.org/10.17159/wsa/2020.v46.i4.9073.

[70] S.C. Chen, C.F. Wan, T.-S. Chung, Enhanced fouling by inorganic and organic foulants on pressure retarded osmosis (PRO) hollow fiber membranes under high pressures, J. Memb. Sci. 479 (2015) 190–203, https://doi.org/10.1016/j.memsci.2015.01.037.

[71] S.C. Chen, G.L. Amy, T.-S. Chung, Membrane fouling and anti-fouling strategies using RO retentate from a municipal water recycling plant as the feed for osmotic power generation, Water Res. 88 (2016) 144–155, https://doi.org/10.1016/j.watres.2015.10.008.

[72] G. Han, P. Wang, T.-S. Chung, Highly robust thin-film composite pressure retarded osmosis (PRO) hollow fiber membranes with high power densities for renewable salinity-gradient energy generation, Environ. Sci. Technol. 47 (2013) 8070–8077, https://doi.org/10.1021/es4013917.

[73] B.D. Coday, D.M. Heil, P. Xu, T.Y. Cath, Effects of transmembrane hydraulic pressure on performance of forward osmosis membranes, Environ. Sci. Technol. 47 (2013) 2386–2393, https://doi.org/10.1021/es304519p.

[74] D.L. Shaffer, J.R. Werber, H. Jaramillo, S. Lin, M. Elimelech, Forward osmosis: where are we now? Desalination 356 (2015) 271–284, https://doi.org/10.1016/j.desal.2014.10.031.

[75] L. Jiang, Z. Tang, K.J. Park-Lee, D.W. Hess, V. Breedveld, Fabrication of non-fluorinated hydrophilic-oleophobic stainless steel mesh for oil-water separation, Sep. Purif. Technol. 184 (2017) 394–403, https://doi.org/10.1016/j.seppur.2017.05.021.

[76] M. Al-Maas, A. Hussain, J. Minier-Matar, D. Ponnamma, M.K. Hassan, M.A.A. Al-Maadeed, K. Alamgir, S. Adham, Validation and application of a membrane filtration protocol for oil-water separation, J. Water Process Eng. (2021), https://doi.org/10.1016/j.jwpe.2021.102185.

[77] B.J. Lee, Y. Zhou, J.S. Lee, B.K. Shin, J.A. Seo, D. Lee, Y.S. Kim, H.K. Choi, Discrimination and prediction of the origin of chinese and korean soybeans using Fourier transform infrared spectrometry (FT-IR) with multivariate statistical analysis, PLoS One 13 (2018) 1–16, https://doi.org/10.1371/journal.pone.0196315.